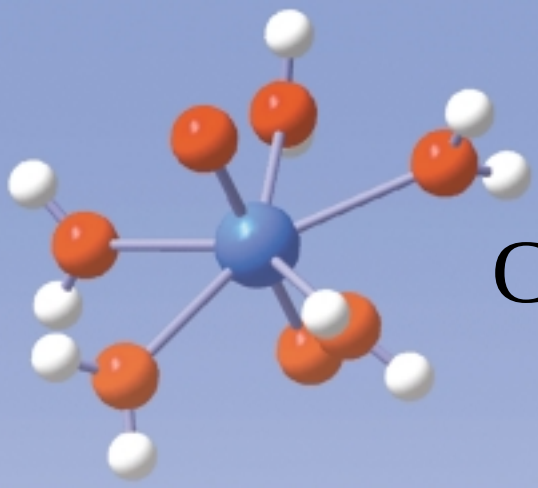

Computational Studies of Actinide Chemistry

P. Jeffrey Hay and Richard L. Martin

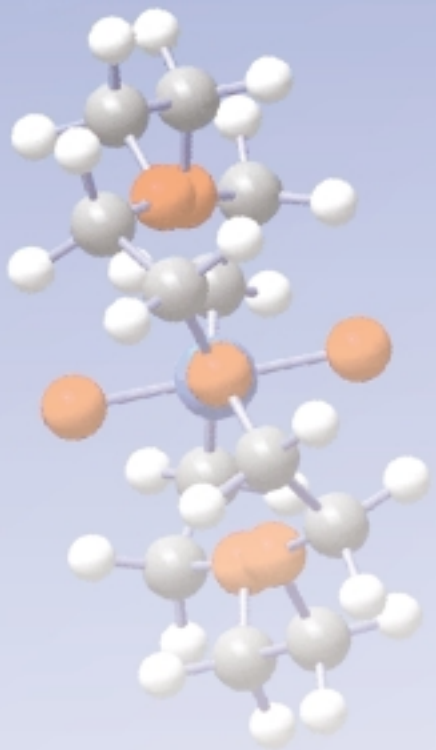

The electronic properties of organic and inorganic molecules can now be calculated from first principles with far greater reliability than has ever been possible. Recent advances in both theory and computation are at the heart of this change. Our Los Alamos group and scientists at other institutions as well have applied the methodology for calculating electronic structure to molecules containing actinide elements. From electronic-structure calculations, one can also compute other molecular properties that can be compared with experimental observations or that can provide information whenever experimental data are absent.

These molecular properties and the corresponding techniques used in determining them experimentally are listed in Table I. For more information on molecular properties, see the articles "The Chemical Complexities of Plutonium" and "XAFS" on pages 364 and 422, respectively.

The ability to perform quantum mechanical calculations on actinide molecules of reasonable size is the result of several factors: steady progress in techniques for solving the molecular Schrödinger equation, tractable approximations to treat relativistic effects, and new approaches in density functional theory (DFT) for calculating properties of chemical interest. We will discuss these issues in greater detail in the next section, but here we will note that the 1998 Nobel Prize in Chemistry recognized the convergence of traditional quantum chemical methodology and DFT. The recipients were John Pople, a pioneer in the development of quantum chemical techniques embodied in the Gaussian electronic-structure codes, and Walter Kohn, one of the founders of DFT.

In the section "Application to Actinyl Species," we illustrate the use of molecular electronic structure calculations on actinide species by examining the series of molecules $AnO_2(H_2O)_5^{2+}$ for the actinide elements (An) uranium, neptunium, and plutonium. Finally, we give an example of an actinide complex, NpO_2(18-crown-6)$^+$, involving an organic ligand to show how DFT enables the study of large molecules containing actinides.

Theoretical and Computational Developments

The first approximation made in treating the quantum mechanics of a set of electrons interacting with a set of nuclei is to "decouple" the electronic motion from the nuclear motion. This is usually a very good approximation because the electrons are much lighter than the nuclei and nearly "immediately" adjust their motion to a

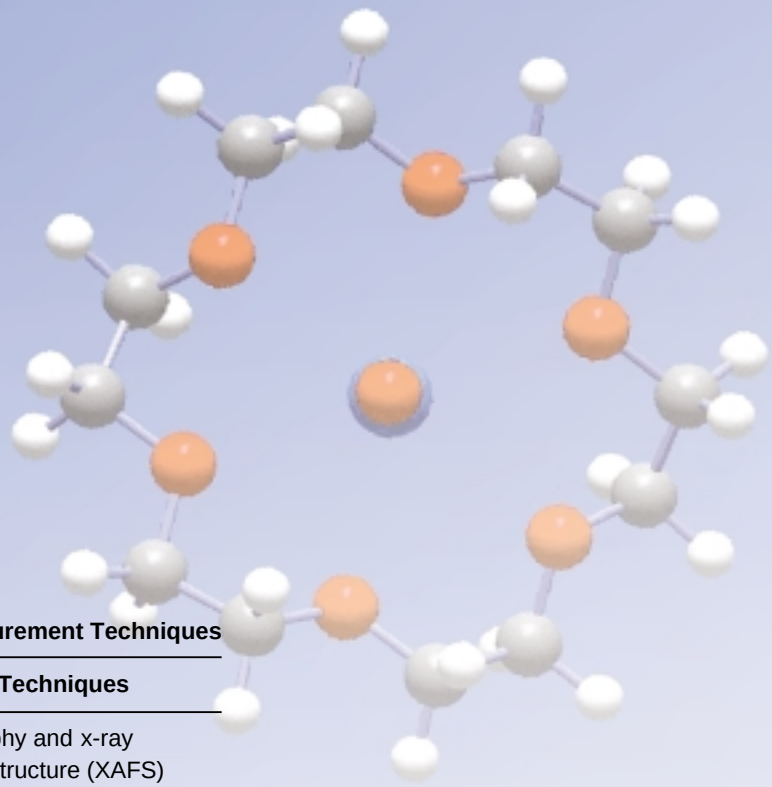

Table I. Molecular Properties and Corresponding Measurement Techniques

Molecular Properties	Measurement Techniques
Bond lengths and angles	X-ray crystallography and x-ray absorption fine-structure (XAFS) spectroscopy
Molecular vibrations	Infrared and Raman spectroscopy
Bond energies and reaction energies	Thermochemical measurements
Activation barriers	Kinetic measurements
Nuclear chemical shifts	Nuclear magnetic resonance (NMR) spectroscopy
Excited electronic states	Visible and ultraviolet spectroscopy

change in the position of the nuclei. We can then write an expression for the electronic energy of the electrons in the fixed electrostatic field of the nuclei:

$$E_e(\mathbf{R}) = E_{kin} + E_{elec-nuc} + E_{elec-elec} \quad . \qquad (1)$$

The energy $E_e(\mathbf{R})$ is written as a function of the fixed nuclear coordinates $\mathbf{R}$, where $\mathbf{R} = (\mathbf{R_1}, \mathbf{R_2}, \ldots, \mathbf{R_N})$ represents the coordinates of all the nuclei in the molecule. The succeeding terms in Equation (1) represent the kinetic energy of the electrons, the attractive interaction between the electrons and the nuclei, and the electron-electron repulsion energy. It is interesting to note that the decoupling of the electronic motion from the nuclear motion is known as the Born-Oppenheimer approximation. It was first introduced by J. Robert Oppenheimer, later to become the first director of Los Alamos, and Max Born, the German physicist and Oppenheimer's postdoctoral advisor (Born and Oppenheimer 1927).

Wave Function Approaches. There are two conceptually distinct approaches to determining the electronic energy in Equation (1): the wave function method and DFT.

In the wave function approach, the electronic Hamiltonian corresponding to the set of electrons and fixed nuclei is written down, and one attempts to solve the Schrödinger equation. The solution, the many-electron wave function, describes the motion of the electrons. It is a function of 3n-variables—*x*, *y*, and *z*—for each of the n electrons in the molecule. Given the many-electron wave function, evaluating the energy and other molecular properties is a straightforward but not a simple process.

The most-basic wave function approximation is to assume that the many-electron wave function is a simple product of one-electron wave functions. This approximation is equivalent to assuming that the motion of each electron is independent of the motion of all the other electrons. As a consequence, an electron feels only the average Coulomb repulsion energy associated with the electron-electron repulsion. The electrons are said to be "uncorrelated" because each is unaware of the detailed positions of the other electrons at any time. Only their average position is felt.

Things are actually a little more complicated because the quantum mechanical requirement that electrons obey Fermi statistics dictates certain symmetry properties when the positions of two electrons are exchanged. This symmetry is satisfied when the simple, independent particle product is generalized to a Slater determinant:

$$\psi_{tot}(\mathbf{r}_1, \mathbf{r}_{2,\ldots,} \mathbf{r}_n) = |\psi_1(\mathbf{r}_1)\psi_2(\mathbf{r}_2)\ldots\psi_n(\mathbf{r}_n)| \quad , \tag{2}$$

where $\psi_i(\mathbf{r})$ are the one-electron molecular orbitals, and ψ_{tot} is the total n-electron wave function. Enforcing this exchange symmetry introduces some correlation in the motion of the electrons—in particular, no two electrons can occupy the same position in space—and leads to a decrease in the electronic energy known as the "exchange" energy. This approach is known as the Hartree-Fock approximation.

Because the Hartree-Fock approximation assumes that the particles are independent, we can write down a separate Schrödinger equation for each electron

$$h_i^{HF}\psi_i(\mathbf{r}) = \varepsilon_i\psi_i(\mathbf{r}) \quad , \tag{3}$$

using the same one-electron Hamiltonian h^{HF} for each electron. The eigenvectors, or molecular orbitals, $\psi_i(\mathbf{r})$ will each have a characteristic orbital energy ε_i. To evaluate the one-electron Hamiltonian h^{HF}, as well as the expressions in the total energy, one needs the total electronic density ρ obtained by adding the densities of the individual orbitals:

$$\rho(\mathbf{r}) = \Sigma_i|\psi_i(\mathbf{r})|^2 \quad . \tag{4}$$

The procedure for obtaining self-consistent solutions to the Schrödinger equation is to guess an initial total density and solve for the molecular orbitals $\psi_i(\mathbf{r})$. We then use these orbitals to determine a new guess for the density and effective Hamiltonian and carry on the calculation until the input density agrees with the output density. The molecular orbitals themselves are usually expanded in a finite Gaussian basis set on each atomic center composed of a radial part, a Gaussian function of the distance from the nucleus, and an angular part, corresponding to various angular momenta (s, p, d, f). The solution to the self-consistent equations involves calculating the one- and two-electron operators over the Gaussian basis set to evaluate the expressions in Equations (1) and (2).

Whereas bond lengths obtained from Hartree-Fock calculations are generally reasonable, bond energies calculated with this method are not accurate enough for the requirements of chemistry. The exchange interaction introduces some correlation in the motion of the electrons, but for reliable bond energies, one must account in a much more detailed way for the explicit correlation between the motion of one and another electron. Several approaches have been developed for including the electron

correlation and for generating increasingly accurate molecular wave functions and electronic energies. Among them are many-body perturbation theory, coupled-cluster theory, and configuration interaction techniques, which typically use the Hartree-Fock wave function as a starting point. These techniques give more accurate results but are computationally even more demanding than Hartree-Fock calculations. As a result, it is difficult to obtain accurate theoretical predictions for moderate to large molecules of interest to experimental chemists.

Developments in Density Functional Theory (DFT). The DFT approach dramatically simplifies the computational demands by replacing the search for an accurate many-electron wave function, which is a function of the coordinates of all the electrons in the molecule, with that for an accurate electronic density, which depends on the coordinates of just a single point in space.

The conceptual foundation of DFT is the Hohenberg-Kohn theorem (Hohenberg and Kohn 1964), which states that knowing the ground-state electronic density suffices in determining all the properties of a many-body system. In the Kohn-Sham electronic-structure formulation of DFT, the electronic energy is partitioned into three terms which are analogous to those in the Hartree-Fock method—the kinetic energy, the electron-nuclei attraction, and the average electron-electron repulsion $\langle E_{\text{elec–elec}} \rangle$. Everything else is lumped into an exchange-correlation energy term:

$$E^{\text{DFT}}(\mathbf{R}) = E_{\text{kin}} + E_{\text{elec–nuc}} + \langle E_{\text{elec–elec}} \rangle + E_{\text{exch–corr}} \quad . \tag{5}$$

Given an expression for $E_{\text{exch–corr}}$, one can formulate one-electron Schrödinger equations analogous to the Hartree-Fock equation, Equation (3), discussed in the previous section. In fact, the Hartree-Fock approximation may be thought of as a specific form of DFT, in which $E_{\text{exch-corr}}$ is approximated by the Hartree-Fock exchange energy. (See the article "Ground-State Properties of the Actinide Elements: A Theoretical Overview" for further details.)

The earliest approximations to the exchange-correlation potential in $E_{\text{exch–corr}}$ were extracted from the properties of the homogeneous electron gas (Kohn and Sham 1965), an approach that worked quite well for describing electrons in metals and was therefore immediately adopted by the physics community. This approach led to an exchange-correlation potential for an electron at some point r, which depended only upon the electronic density at point r, $\rho(r)$. It became known as the local density approximation (LDA). But LDA significantly overestimates bond energies. In the past few years, however, functionals called generalized gradient approximations, or GGA, have been developed (Perdew 1986, Becke 1988), in which the exchange-correlation energy $E_{\text{exch–corr}}$ depends on the local density and its gradient, thereby introducing some inhomogeneity and nonlocality. Even more recently, additional improvements in bond energies have been obtained with hybrid density functionals (Becke 1993), which contain a portion of the full, nonlocal Hartree-Fock exchange interaction discussed earlier in the context of the wave function approaches.

The tremendous simplification afforded by DFT arises from the fact that all the expressions depend only on an accurate knowledge of the density in three spatial dimensions. It is this feature that allows DFT to be applied to much larger molecules than is possible with approaches based on Hartree-Fock, which were described earlier. This simplification is especially important when one considers the $E_{\text{exch–corr}}$ term described before, which incorporates the electron correlation effects. By contrast, Hartree-Fock-based methods for treating electron correlation typically include expressions involving all the occupied and unoccupied orbitals. The combination of improved functionals and computational advances has now enabled chemists to routinely apply DFT methods to the electronic structure of molecules of ever-increasing complexity.

Relativistic Effective Core Potentials (RECPs). The final ingredient for our specific approach to actinide chemistry is the use of RECPs. In molecules containing heavy atoms, such as the actinides, the motion of the electrons must be treated relativistically because the effective velocity of the electrons (especially the inner core electrons that penetrate closer to the nucleus) is nonnegligible relative to the speed of light. In the Schrödinger equation for a valence orbital, Equation (3), the one-electron Hamiltonian *h*,

$$h = T + V_{\text{core}} + V_{\text{nuc}} + V_{\text{rel}} + V_{\text{val}} \quad , \tag{6}$$

includes the kinetic energy of the electron (*T*), the interactions with the nucleus and the core electrons ($V_{\text{core}} + V_{\text{nuc}}$), the interactions with the other valence electrons (V_{val}), and the relativistic operator (V_{rel}), which contains the so-called "mass-velocity" and "Darwin" operators. With the RECP, the Schrödinger equation becomes

$$h = T + V_{\text{RECP}} + V_{\text{val}} \quad . \tag{7}$$

The RECP in Equation (7) serves to replace the Coulomb effects of the inner core electrons on the valence electrons, as well as the direct relativistic effects on the valence electrons. RECPs can be used in either Hartree-Fock or DFT approaches to studies of molecules containing heavier elements. As a rule, relativity has a noticeable effect on the electronic levels and, in turn, on calculated molecular bond lengths and bond energies for elements beyond krypton (Z > 36). This range includes the second and third transition-metal series, as well as the lanthanides and actinides. The effects of spin-orbit coupling, which also arises from relativistic interactions, must be included directly in any calculation.

The procedures for generating RECPs for heavy atoms were developed by Jeffrey Hay and Willard Wadt (1985). The initial impetus for these developments came from the programmatic effort at Los Alamos to study actinide molecules for laser isotope separation. We calculated the electronic structure of uranium hexafluoride (UF_6), plutonium hexafluoride (PuF_6), and related molecules, using "first-generation" RECPs for uranium and plutonium (Hay et al. 1979, Hay 1983, Wadt 1987). A set of RECPs for 56 main-group and transition-metal elements of the periodic table was published (Hay and Wadt 1985) and disseminated to the quantum-chemistry community. The methodology for manipulating RECPs developed by Richard Martin, Larry McMurchie, and Ernest Davidson has been incorporated into the Gaussian codes for performing quantum-chemistry calculations developed by John Pople and his collaborators over the past twenty years. Following these developments, investigators throughout the world have been using both Hartree-Fock and DFT approaches to treat heavy-atom chemistry by using RECPs. More recently, we have developed a set of "second-generation" RECPs (Hay and Martin 1998) and have employed them in our studies of actinide molecules (Hay and Martin 1998, Schreckenbach et al. 1998) by using the DFT approaches described in this article.

Application to Actinyl Species

Electronic Structure of Actinyl Complexes. In this section, we present DFT results for the structures and properties of a typical actinyl species in solution denoted generically as $AnO_2\ (H_2O)_5^{2+}$, where An is uranium, neptunium, or plutonium. These molecules, all of which contain the common AnO_2^{2+} unit surrounded by five water molecules, are the commonly observed species involving the An(VI) oxidation

Table II. Analysis of the Electronic Structure of $UO_2(H_2O)_5^{2+}$ from a Simplistic "Ionic" Picture and from DFT Calculations

Occupied Orbitals in Neutral Atoms	Charge on Each Entity				Occupation of Atomic Orbitals	
	Ionic Model		DFT Results		Ionic Model	DFT Results
U $6s^2 6p^6 5f^3 6d^1 7s^2 7p^0$	U	+6.0	U	+1.66	U $6s^2 6p^6 5f^0 6d^0 7s^0 7p^0$	U $6s^2 6p^6 5f^{2.71} 6d^{1.26} 7s^{0.21} 7p^{0.16}$
O $2s^2\ 2p^4$	O	–2	O	–0.26	O $2s^2\ 2p^6$	O $2s^{1.94}\ 2p^{4.32}$
	H_2O	0.0	H_2O	+0.18		

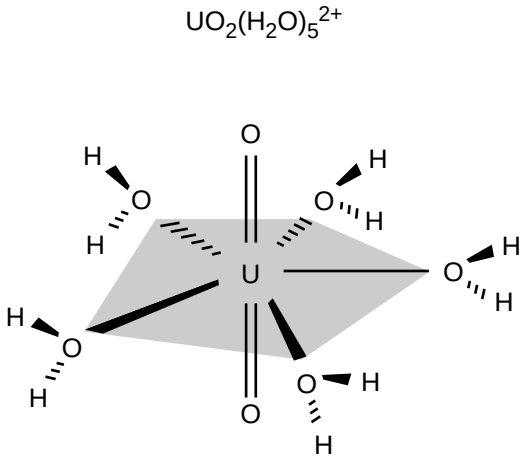

Figure 1. Schematic of the Geometric Structure of $UO_2(H_2O)_5^{2+}$
The linear O=U=O uranyl is oriented vertically, and the five water molecules are coordinated to the uranium atom in the equatorial plane. The hydrogen atoms of the equatorial water molecules are oriented in such a way as to lie roughly perpendicular to the equatorial plane.

state in solution at low pH. Shown in Figure 1 is a schematic representation of the uranyl complex.

The electronic properties of the molecule are determined primarily by the AnO_2^{2+} actinyl unit because the water molecules act essentially as neutral ligands coordinated to the metal. The electronic structure of AnO_2^{2+}, in turn, is closely tied to the orbitals of the actinide atom. For the case of UO_2^{2+}, it is useful to consider an extreme "ionic" picture as a starting point for thinking about the electronic structure although this picture turns out to be somewhat unrealistic for describing the true electronic density of the molecule, as we will discuss shortly. In this picture, the oxygen atoms are treated as O^{2-}, and the uranium atom is treated as U^{6+}. Each atom has adopted a closed-shell configuration. As shown in Table II, the O^{2-} ions adopt the inert gas $2s^2 2p^6$ configuration, and all the atomic levels in the U^{6+} ion are filled up through the 6s and 6p shells. (The radial functions of the actinide atoms are shown in the article "The Chemical Complexities of Plutonium" on page 364.) The 5f, 6d, and higher levels are formally empty in this picture. Based upon this picture, one would also anticipate a $UO_2(H_2O)_5^{2+}$ molecule with no unpaired electrons, as is indeed found to be the case in the ground-state solution of the electronic structure.

For the neptunium and plutonium counterparts of this species, we recall that the atomic state of Np^{6+} has a filled $6s^2 6p^6$ core as does U^{6+}, but it also has one unpaired electron in the 5f orbital. Similarly, the atomic state of Pu^{6+} has a $5f^2$ configuration with two unpaired electrons. The same is true of the molecular calculations, in which the ground states have one unpaired electron with spin = 1/2 for $NpO_2(H_2O)_5^{2+}$ and two unpaired electrons with spin = 1 for $PuO_2(H_2O_5)^{2+}$.

When the molecular orbitals are calculated self-consistently, a picture of the bonding emerges that is much more covalent when compared with the ionic model for the uranyl UO_2^{2+} entity, which has +6 and –2 charges on the uranium and oxygen,

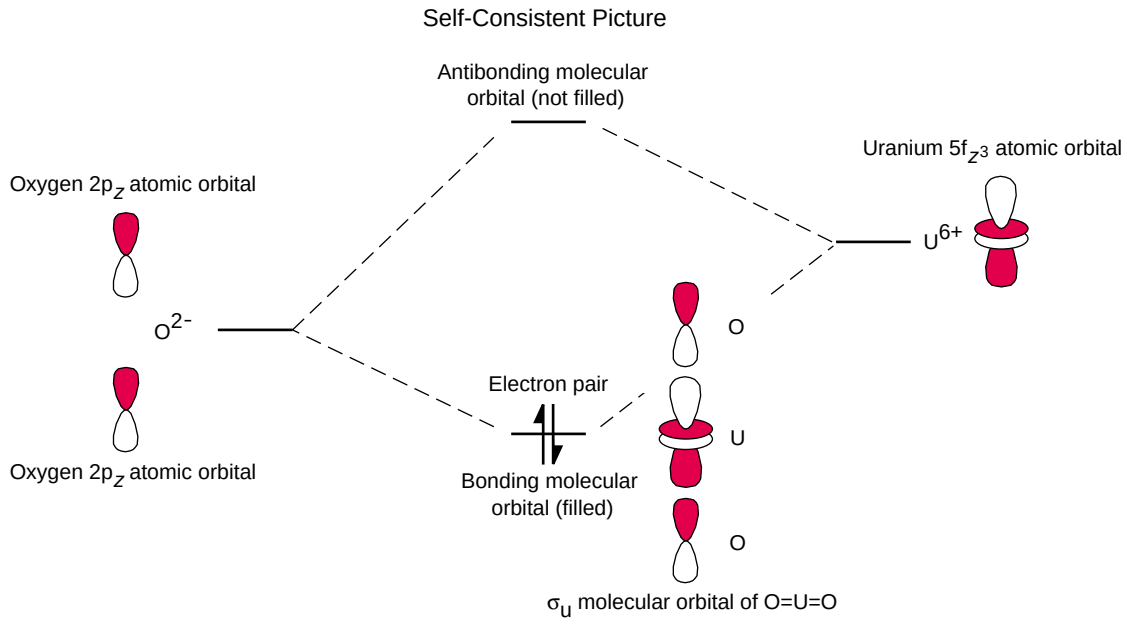

Figure 2. Formation of a Bonding σ_u Molecular Orbital
The figure shows the interaction of two oxygen 2p$_z$ orbitals (left) in the uranyl unit with the uranium 5f$_{z^3}$ orbital (right) to form a bonding σ_u molecular orbital (center) in the O=U=O bond. The figure also suggests the energy levels (solid lines) of the atomic orbitals relative to the energy levels of the molecular orbitals in the self-consistent picture.

respectively. An analysis of the DFT results for $UO_2(H_2O)_5^{2+}$ shows that the resultant charge distribution is closer to +1.66 for uranium and –0.26 for each oxygen in the uranyl group (see Table II). Some residual charge (+0.18) remains on each of the equatorial water molecules. This change is evident in the six molecular orbitals describing the uranyl bond. In the ionic picture, these orbitals would be strictly atomic in character and would involve the $2p_x$, $2p_y$, and $2p_z$ orbitals on each of the oxygen atoms. Using the symmetry designations of O=U=O, we denote these orbitals σ_g, σ_u, π_{ux}, π_{uy}, π_{gx}, and π_{gy}. One of the most important contributions arises from the σ_u orbital, which involves not only the $2p_z$ atomic orbitals of the oxygen atoms but also the $5f_{z^3}$ orbital of the uranium atom. In Figure 2, the atomic orbitals of each atom are shown before they interact, as we assumed in the ionic model. In the middle of Figure 2, the molecular orbital is shown schematically in order to illustrate bonding interactions of the oxygen $2p_z$ orbitals with the uranium $5f_{z^3}$ orbital.

We now turn to another aquo complex, $PuO_2(H_2O)_5^{2+}$, which is qualitatively similar to $UO_2(H_2O)_5^{2+}$. As mentioned before, unlike its uranium counterpart, the plutonium complex has two unpaired electrons in the $5f_{xyz}$ and $5f_{x(x^2-y^2)}$ molecular orbitals. These molecular orbitals are essentially identical to the atomic $5f_{xyz}$ and $5f_{x(x^2-y^2)}$ orbitals of plutonium. The calculated optimum structure from DFT results is shown in Figure 3(a), which closely resembles the schematic drawing of aquo complexes in Figure 1. A contour plot in Figure 3(b) shows the positive and negative amplitudes of the self-consistent molecular orbital most closely corresponding to the σ_u molecular orbital of the isolated O=Pu=O group. The constructive interference of the bonding interaction between the oxygen $2p_z$ orbitals and the plutonium $5f_{z^3}$ orbital, which was sketched in Figure 2, now actually appears as a single contour in the figure. As already mentioned, there are five other molecular orbitals representing the 12 electrons in the O=An=O bonds, in which the 5f and 6d orbitals on the actinide can participate, but we will not discuss these other orbitals in detail here.

Properties of Aquo and Crown Complexes of Actinyl Species. In this section, we discuss the geometries and other properties of actinyl complexes obtained from DFT calculations. To obtain the optimized structure, we vary the total molecular energy $E^{DFT}(\mathbf{R})$, which was discussed in the section "Theoretical and Computational Developments," as a function of all the nuclear coordinates until a stable, or minimum-energy, solution is found. Table III compares the calculated bond lengths

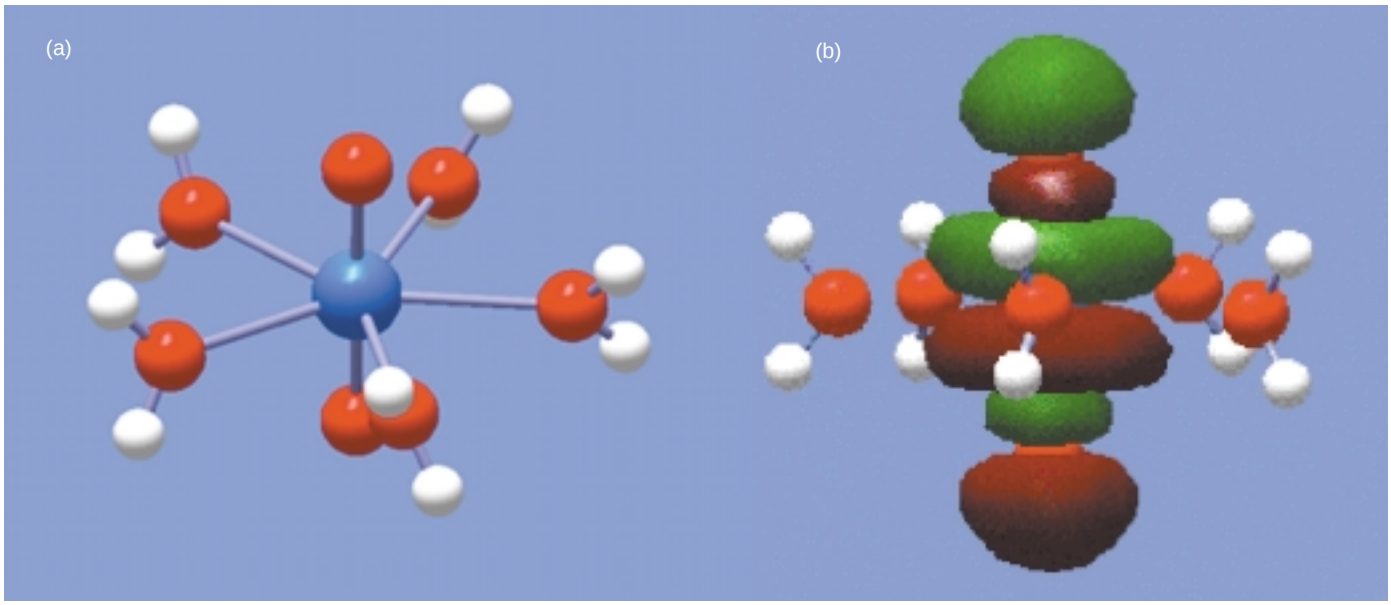

Figure 3. Structure of $PuO_2(H_2O)_5^{2+}$ and a Bonding Molecular Orbital of PuO_2
(a) The structure of $PuO_2(H_2O)_5^{2+}$, as determined from quantum chemical DFT calculations, is shown on the left, where the colored spheres indicate plutonium (blue), oxygen (red), and hydrogen (white). (b) Shown here is a contour plot of one of the occupied bonding molecular orbitals of the O=Pu=O unit, where positive and negative amplitudes are depicted as green and brown, respectively. The plotted orbital resembles most closely the σu orbital of PuO_2^{2+}. The plot shows the participation of the $5f_{z^3}$ atomic orbital on the plutonium atom and of the $2p_z$ atomic orbital on the oxygen atoms. Relatively little participation is evident from the atomic orbitals of the equatorial atoms.

from DFT with experimentally measured quantities from XAFS spectroscopy in solution. As shown in the table, there is good agreement between the theoretical calculations and the measured values for the actinyl bond: both find a bond length of 1.76 angstroms for U=O, 1.75 angstroms for Np=O, and 1.74 angstroms for Pu=O. By contrast, the Hartree-Fock results predict that the U=O bond length is substantially shorter (1.69 angstroms). In the case of the uranyl complex, for the longer equatorial bonds to the water molecules, DFT predicts a slightly longer bond length (2.51 angstroms) compared with experiment (2.42 angstroms).

The vibrational frequencies are calculated from the curvature (second derivatives) of $E^{DFT}(\mathbf{R})$ about the minimum-energy geometry with respect to the nuclear coordinates. The two modes corresponding to the symmetric and antisymmetric motion (denoted ν_s and ν_{as}, respectively, in Table III) of the O=U=O atoms are the most characteristic vibrational fingerprint of the molecule. These two modes can be detected by Raman and infrared vibrational spectroscopy, respectively. The symmetric stretch is predicted to lie at lower energy than the antisymmetric stretch (908 cm^{-1} versus 1001 cm^{-1}), and this prediction agrees with the experimental data.

The structural comparisons (Table III) show a slight contraction (namely, by 0.01 angstrom) of the actinyl bond as one goes down the actinide series from uranium to neptunium and then to plutonium. This trend is fairly typical in actinide compounds and is often called the actinide "contraction," analogous to the lanthanide contraction found in the 4f series. Similarly, one also finds a slight progressive decrease in the neptunium-water and plutonium-water bond lengths.

Although we have focused on just a few features of the results of electronic-structure calculations—those that allow comparisons with experiment—the calculations provide other useful information, which can be difficult to measure. For example, the calculations automatically give the frequencies of all 48 vibrations. Using these theoretical techniques, one can also look at questions in solution chemistry that can be difficult or too ambiguous to measure experimentally. Such issues include how much energy is involved in binding additional water molecules to the central actinyl species, the relative energies in binding water compared with other ligands, such as hydroxide (OH^-) or halide (Cl^-), and the activation barriers that must be surmounted in chemical reactions. In fact, calculations by Schreckenbach et al. (1998) have shown that the uranyl bond can exist under the right circumstances in a bent form, with O=U=O bond angles ranging from 115° to 130°, whereas all known forms of

Table III. Bond Lengths and Vibrational Frequencies from DFT and Hartree-Fock (HF) Calculations and from Experimental Results for $AnO_2(H_2O)_5^{2+}$ Complexes

	$UO_2(H_2O)_5^{2+}$ Spin = 0			$NpO_2(H_2O)_5^{2+}$ Spin = 1/2		$PuO_2(H_2O)_5^{2+}$ Spin = 1	
	Methodology						
	HF	DFT	XAFS	DFT	XAFS	DFT	XAFS
Bond Length							
R(An=O) (Å)	1.69	1.76	1.76	1.752	1.75	1.742	1.74
R(An–OH_2) (Å)	2.54	2.51	2.42	2.50	2.42	2.485	2.41
	HF	DFT	Raman, IR	DFT	Raman, IR	DFT	Raman, IR
Stretch Frequency							
ν_s (cm^{-1})	1091	908	872	854	863	805	835
ν_{as} (cm^{-1})	1149	1001	965	983	969	951	962

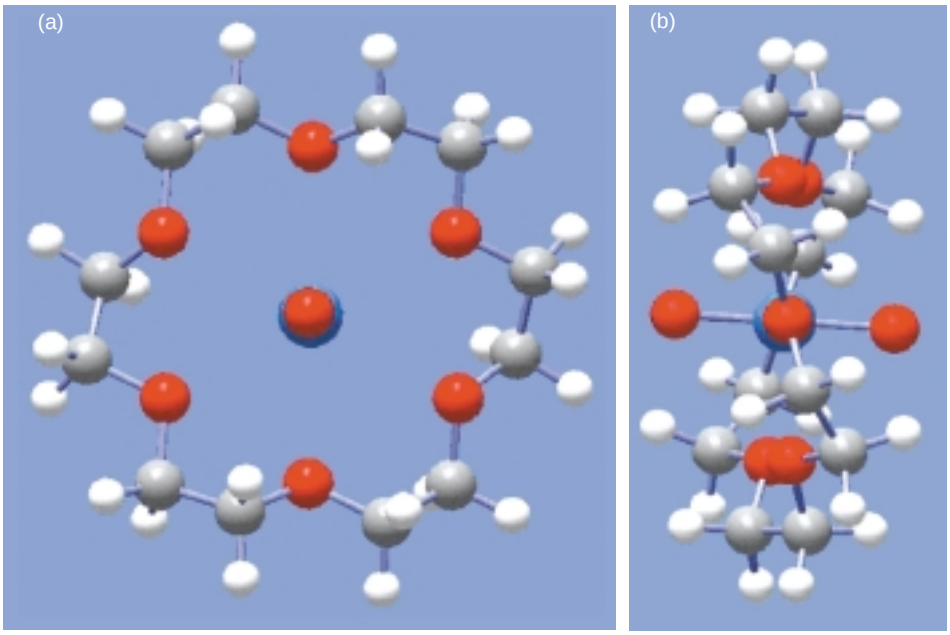

Figure 4. Predicted Atomic Positions in the $NpO_2(18\text{-crown-}6)^+$ Complex
Shown here are the top (a) and side (b) views of the calculated atomic positions in the complex $NpO_2(18\text{-crown-}6)^+$ as determined from quantum chemical DFT calculations. The spheres indicate neptunium (blue), oxygen (red), carbon (gray), and hydrogen (white).

uranyl complexes have linear O=U=O bonds (180°). It remains to be seen if such species can actually be isolated as stable compounds.

All the previous results have been obtained while ignoring the interactions of the actinide species with the surrounding aqueous solution. In order to compare these results with those from experimental measurements in solution, we must include solvent effects on the molecular energies obtained by DFT or other techniques. A discussion of these techniques, however, would take us beyond the scope of this article. We will mention briefly that we have been investigating solvent effects in collaboration with Lawrence Pratt of Los Alamos (Martin et al. 1998). These interactions can often be successfully incorporated when we treat the interaction of the molecular wave functions with a classical "dielectric" model for the surrounding medium. Depending on the overall charge of the actinide species, these solvent effects can be very large (100–200 kilocalories per mole) for energies of reaction in solution,

and they must be included for complete comparisons with experiment.

These theoretical capabilities, together with the experimental characterization techniques described in the main article, now offer a powerful combination for unraveling the complexities of actinide chemistry. Figure 4 is an illustration of the results of our recent DFT calculation on a much larger neptunyl(V) complex with an organic ether, 18-crown-6, that contains six oxygen atoms. The crown ether molecule has been observed (Clark et al. 1998) experimentally to bind to the neptunium along the equator of the neptunyl bond in a manner similar to that of the water molecules in our previous case. The predicted Np=O bond length of 1.814 angstroms agrees well with the measured value of 1.800 angstroms. The same good agreement is true of the predicted frequency value (776 cm^{-1}) and the results obtained by Raman spectroscopy (780 cm^{-1}). Calculations have now predicted the structural and vibrational properties of crown ether complexes of uranium, neptunium, and plutonium in both +6 and +5 oxidation states, as well as ligand binding energies in solution. All these findings illustrate how the new DFT methodologies, coupled with constantly improving computational capabilities, enable theory to make predictions on large actinide molecules of experimental interest. ■

Jeffrey Hay received a B.A. in chemistry from Franklin and Marshall College in 1967 and a Ph.D. in chemistry from the California Institute of Technology in 1972. He has been a staff member in the Theoretical Division at Los Alamos since 1974 and was named a Laboratory Fellow in 1992. Hay is the author of more than 100 articles in refereed journals. His research interests include the electronic structure and chemistry of transition-metal and actinide compounds and applications of quantum chemistry and cluster approaches to problems in heterogeneous catalysis and materials chemistry.

Richard Martin received his B.S. in chemistry (magna cum laude) from Kansas State University and a Ph.D. in chemistry from the University of California, Berkeley. He spent two years as a Chaim Weizmann fellow with Ernest Davidson at the University of Washington before joining the theoretical chemistry and molecular physics group at Los Alamos in 1978. His research interests are in the general area of electronic-structure theory, particularly as applied to the description of transition-metal and actinide systems.

Further Reading

Becke, A. D. 1988. *Physical Review A* **37**: 3098.

Becke, A. D. 1993. *Journal of Chemical Physics* **98**: 5648.

Born, M., and J. R. Oppenheimer. 1927. *Annalen Physik* **84**: 457.

Clark, D. L., D. W. Keogh, P. D. Palmer, B. L. Scott, and C. D. Tait. 1998. *Angewandte Chemie—International Edition* **37**: 164.

Hay, P. J. 1983. *Journal of Chemical Physics* **79**: 5469.

Hay, P. J., and R. L. Martin. 1998. *Journal of Chemical Physics* **109**: 3875.

Hay, P. J., and W. R. Wadt. 1985. *Journal of Chemical Physics* **82**: 270.

Hay, P. J., 1979. *Journal of Chemical Physics* **70**: 1767.

Hohenberg, P., and W. Kohn. 1964. *Physical Review B* **136**: 864.

Kohn, W., and L. J. Sham. 1965. *Physical Review A* **140**: 113.

Martin, R. L., L. R. Pratt, and P. J. Hay. 1998. *Journal of Physical Chemistry A* **102**: 3565.

Perdew, J. P. 1986. *Physical Review B* **33**: 8922.

Schreckenbach, G., P. J. Hay, and R. L. Martin. 1998. *Inorganic Chemistry* **37**: 4442.

Wadt, W. R. 1987. *Journal of Chemical Physics* **86**: 339.